^{14}N Nuclear Quadrupole Coupling and Methyl Internal Rotation of 2-, 4-, and 5-Methyl Oxazole

Eckhard Fliege, Helmut Dreizler, and Michael Meyer

Abteilung Chemische Physik im Institut für Physikalische Chemie, Christian-Albrechts-Universität, Olshausenstraße 40, D-2300 Kiel

Khalid Iqbal * and John Sheridan

School of Physical and Molecular Sciences, University College of North-Wales, Bangor, Gwynedd LL57 2UW, U.K.

Z. Naturforsch. **41 a**, 623–636 (1986); received December 16, 1985

In the following we give an outline of ^{14}N nuclear quadrupole, internal axis method (IAM) methyl internal rotation, and fourth order centrifugal distortion – only needed for extrapolating transition frequencies to higher J values – analyses performed for 2-, 4-, and 5-methyl oxazole.

The results are discussed, the three methyl oxazoles being compared with one another and with their common parent, oxazole.

Introduction

After a comprehensive study of the five-membered heterocyclic ring molecule oxazole comprising a determination of the complete r_s-structure [1] and the principal quadrupole coupling tensor [2] had been completed at Bangor, the spectroscopic investigations were extended to its three isomeric monomethyl derivatives [3]. This was done with the objective to examine the influence of methyl substitution on the principal ^{14}N quadrupole coupling tensor, and secondly to study the variation of the potential hindering methyl internal rotation at the different heterocyclic ring positions. This work follows the essentially similar treatment of the case of isoxazole and its monomethyl derivatives [4].

The rotational spectra were assigned at Bangor using a conventional 100 kHz Stark-effect modulated spectrometer and starting with rotational constants from an assumed structure which consisted of the oxazole r_s-structure [1] and a plausible methyl configuration. The fact that most lines are split by a few up to some tens of MHz due to internal rotation, and a closer look at the Stark lobes facilitated the assignment.

Later, it seemed worthwhile remeasuring the spectra with a microwave Fourier transform (MWFT) spectrometer at Kiel in order to get the ^{14}N quadrupole hyperfine structure (^{14}N-hfs) resolved and to obtain more accurate torsional A-E splittings. Many investigations up to now have proved MWFT spectroscopy to be a powerful sensitive tool for a precise measurement of line frequencies and for the resolution of narrow splittings. The fine and hyperfine structure analyses reported in this paper are therefore based on these measurements.

Experimental

The samples of 2- and 5-methyl oxazole were kindly provided by Dr. R. Hull and Prof. Dr. U. Schöllkopf, Göttingen, respectively. The 4-methyl oxazole was prepared according to Cornforth and Cornforth [5]. A further sample of 5-methyl oxazole was synthesized using a method of preparation proposed by Prof. Dr. U. Schöllkopf, Göttingen, proceeding from methyl isocyanide [3, 6].

In Bangor the microwave spectra of the three isomeric methyl oxazoles have been measured with conventional 100 kHz Stark-effect modulation at sample gas pressures down to 5 mTorr and temperatures near 20 °C in the frequency range of 15–40 GHz. In Kiel we did the measurements with MWFT spectrometers in J- [7], X- [8], and Ku- [9] band, i.e.

* Present Address: Al Serat Trust, Ahmed Pur East, Pakistan.

Reprint requests to Prof. Dr. H. Dreizler, Abteilung Chemische Physik im Institut für Physikalische Chemie, Christian-Albrechts-Universität, Olshausenstr. 40, D-2300 Kiel, F.R.G.

0340-4811 / 86 / 0400-0623 $ 01.30/0. – Please order a reprint rather than making your own copy.

from about 5 GHz to 18 GHz, at pressures below 1 mTorr and a temperature of about −70 °C.

In the case of 5-methyl oxazole μ_a- as well as μ_b-transitions were recorded at Kiel, whereas for 2- and 4-methyl oxazole we looked only for rotational transitions due to the stronger dipole moment component, i.e., μ_b-lines (see Table 1). The first set of measurements of the latter two molecules had later to be supplemented in order to obtain a satisfactory fit of all three internal rotation parameters including the angle $\sphericalangle(a, i)$ between the internal rotation axis i and the principal inertial axis a. The angle $\sphericalangle(a, i)$ is needed for a comparison of the principal electric field gradient tensors at nitrogen-^{14}N in oxazole and in the methyl substituted species (see Section "Discussion" in this paper). One of us (M.M.) did these supplementary measurements in J- and X-band, i.e., in the frequency range of 5−12 GHz. An example of the MWFT recordings is given in Figure 1. The measured rotational lines with their methyl torsional A and E fine structure and their ^{14}N-hfs components are listed in Tables 2a−c.

Table 1. Dipole moment components in the direction of the principal inertial axes a and b and total dipole moments. The dipole moments are given in Debye (1 D ≙ 10^{-18} esu) and in SI-units using the relation

$$1\ \mathrm{D} = 10^{-18}\ \mathrm{esu} = 3.3356 \cdot 10^{-30}\ \mathrm{kg^{1/2}\,m^{5/2}\,sec^{-1}} = 3.3356 \cdot 10^{-30}\ \mathrm{Asecm}.$$

Single standard errors in brackets.

μ_a [D]	μ_a [Asecm] · 10^{31}	μ_b [D]	μ_b [Asecm] · 10^{31}	μ_{total} [D]	μ_{total} [Asecm] · 10^{31}
2-Methyl oxazole					
0.27(5)	9.0(17)	1.35(5)	45.0(17)	1.37(7)	45.7(23)
4-Methyl oxazole					
0.22(4)	7.3(13)	1.06(4)	35.4(13)	1.08(5)	36.0(17)
5-Methyl oxazole					
2.08(5)	69.4(17)	0.60(4)	20.0(13)	2.16(4)	72.0(13)

Stark effect measurements were also made at Bangor [3] on all three substances, by the conventional method of applying a static electric field of up to several hundred volts per centimeter to the Stark effect electrode in a calibrated X-band cell. The transitions selected were: for 2-methyl oxazole $4_{04}-3_{13}$; for 4-methyl oxazole $2_{21}-1_{10}$; and for 5-methyl oxazole $3_{03}-2_{02}$, $3_{12}-2_{11}$ and $4_{04}-3_{03}$. Good linear plots of frequency displacements ($\Delta\nu$)

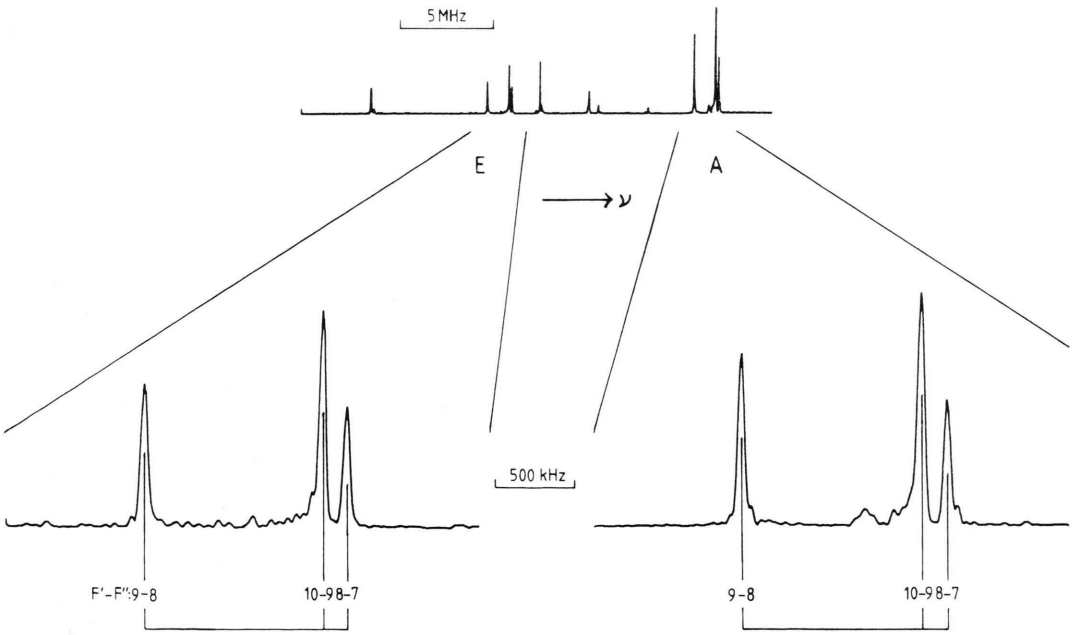

Fig. 1. Methyl torsional fine and nitrogen-^{14}N hyperfine structure of the $9_{28}-8_{35}$ transition of 2-methyl oxazole. *Upper trace:* A 25 MHz scan of the rotational spectrum recorded with MWFT spectroscopy. Power spectrum, sample interval: 20 nsec, 1280 k cycles, 1024 data points supplemented by 3072 zeros; microwave polarizing frequency: 15797 MHz, sample gas pressure: 0.6 mTorr, temperature in the waveguide cell: −70 °C. − *Lower traces:* Two ranges of 3 MHz of the upper trace recording with the E- and A-species torsional satellite respectively. The expected intensities of the ^{14}N-hfs components have been plotted as stroke pattern below the respective torsional satellite.

Table 2. Measured transitions of 2-, 4- and 5-methyl oxazole. Γ: Symmetry species, ν_{exp}: experimental frequency, $\Delta\nu_{hfsA}$: measured A-species ^{14}N-hfs shift related to the most intense component, $\Delta\nu_{AE}$, $\Delta\nu_{AE\#}$: experimental torsional splitting A−E and A−E# with E#: forbidden E-species line (standard deviation from averaging the hfs components in kHz in brackets), $\overline{\nu_{0A}}$: centre frequency for the rotational A-species line (see text), $\delta_{calc-exp}$: difference between calculated and experimental frequency or splitting, *: transition not used for ^{14}N-quadrupole hfs analysis, **: not used for methyl internal rotation analysis, nm: not measured; frequencies, splittings and deviations in MHz. The rotational level with the higher energy value is $J'\ K'_-\ K'_+$.

Table 2a. Measured transitions of 2-methyl oxazole.

J'	K'_-	K'_+-J''	K''_-	K''_+	$F'-F''$	Γ	ν_{exp}	$\Delta\nu_{hfsA}$	$\delta_{calc-exp}$	$\Delta\nu_{AE}$ / $\Delta\nu_{AE\#}$	$\delta_{calc-exp}$	$\overline{\nu_{0A}}$	$\delta_{calc-exp}$
1	1	0 − 1 *	0	1	2 − 2	A	6444.144			−15.248(32)	0.230	6444.178	0.002
						E	6459.410						
					1 − 1	A	6444.344	−0.200	0.028				
						E	nm						
					2 − 1	A	6443.685	0.459	0.004				
						E	6458.974						
					1 − 2	A	6444.774	−0.630	−0.005				
						E	6459.980						
					0 − 1	A	6442.729	1.415	0.001				
						E	6457.959						
1	1	1 − 0	0	0	2 − 1	A	11812.592			55.659(56)	−0.068	11812.408	0.028
						E	11756.941						
					1 − 1	A	11811.491	1.101	−0.003				
						E	11755.896						
					0 − 1	A	11814.240	−1.648	0.001				
						E	11758.509						
2	0	2 − 1 *	1	1	3 − 2	A	7256.447			−55.173(49)	0.128	7256.703	0.016
						E	7311.617						
					2 − 1	A	7257.872	−1.425	−0.003				
						E	7312.985						
					1 − 0	A	7254.618	1.829	0.002				
						E	7309.867						
					2 − 2	A	nm						
						E	7311.921						
					1 − 1	A	7257.363	−0.916	0.002				
						E	7312.522						
2	1	2 − 1	0	1	3 − 2	A	17180.865			32.331(3)	0.077	17180.634	0.044
						E	17148.532						
					2 − 1	A	17179.717	1.148	−0.005				
						E	17147.389						
2	2	0 − 1 *, **	1	1		A	31235.82			−280.47	−17.84	31235.82	0.08
						E	31516.29						
2	2	1 − 1 *, **	1	0		A	30068.96			391.31	27.74	30068.96	−0.15
						E	29677.65						
2	1	1 − 2 *	0	2	3 − 3	A	7611.074			7.574(5)	0.180	7611.267	−0.005
						E	7603.505						
					2 − 2	A	7611.929	−0.855	0.009				
						E	7604.351						
					1 − 1	A	nm						
						E	7603.038						
2	2	0 − 2	1	1	3 − 3	A	16368.218			nm		16367.880	0.041
					2 − 2	A	16366.710	1.508	−0.001				
					1 − 1	A	16369.048	−0.830	−0.007				
3	0	3 − 2	1	2	4 − 3	A	14168.009			−30.080(5)	−0.080	14168.185	0.028
						E	14198.089						
					3 − 2	A	14168.791	−0.782	−0.002				
						E	14198.865						
					2 − 1	A	14167.592	0.417	−0.003				
						E	14197.679						
3	1	3 − 2 *, **	0	2		A	22087.64			25.93	0.28	22087.64	−0.01
						E	22061.71						
3	1	2 − 3	0	3	4 − 4	A	9592.686			12.188(6)	0.291	9592.977	−0.017
						E	9580.493						
					3 − 3	A	9593.868	−1.182	−0.003				
						E	9581.676						
					2 − 2	A	9592.257	0.429	−0.014				
						E	9580.078						

Table 2a (continued)

J'	K'_-	K'_+-J''	K''_-	K''_+	$F'-F''$	Γ	ν_{exp}	$\Delta\nu_{hfsA}$	$\delta_{calc-exp}$	$\Delta\nu_{AE}$ / $\Delta\nu_{AE\#}$	$\delta_{calc-exp}$	$\overline{\nu_{0A}}$	$\delta_{calc-exp}$
3	2	1 − 3	1	2	4 − 4	A	15431.339			−110.540(40)	0.596	15431.117	0.037
						E	15541.892						
					3 − 3	A	15430.457	0.882	−0.004				
						E	15540.942						
					2 − 2	A	15431.643	−0.304	−0.003				
						E	15542.224						
3	2	2 − 3 *, **	1	3		A	20960.55			226.34	2.02	20960.55	0.10
						E	20734.21						
4	0	4 − 3 *, **	1	3		A	20972.79			−20.70	−0.26	20972.79	0.08
						E	20993.49						
4	1	3 − 3	2	2	5 − 4	A	12591.496			−236.801(63)	0.168	12591.835	−0.019
						E	12828.315						
					4 − 3	A	12592.790	−1.294	0.026				
						E	12829.507						
					3 − 2	A	12591.147	0.349	−0.023				
						E	12828.014						
4	1	4 − 3 *, **	0	3		A	26707.07			22.93	−0.05	26707.07	−0.16
						E	26684.14						
4	1	3 − 4	0	4	5 − 5	A	12579.255			12.125(16)	0.522	12579.617	−0.028
						E	12567.109						
					4 − 4	A	12580.667	−1.412	−0.022				
						E	12568.546						
					3 − 3	A	12578.846	0.409	−0.040				
						E	12566.738						
4	2	2 − 4	1	3	5 − 5	A	14788.559			nm		14788.455	0.027
					4 − 4	A	14788.154	0.405	0.003				
					3 − 3	A	14788.674	−0.115	0.010				
4	2	3 − 4 *, **	1	4		A	23159.83			126.11	1.27	23159.83	0.20
						E	23033.72						
4	4	0 − 5 *	3	3	5 − 6	A	8916.706			125.040(36)	−0.267	8916.459	0.028
						E#	8791.678						
					4 − 5	A	8915.784	0.922	−0.012				
						E#	8790.695						
					3 − 4	A	8916.934	−0.228	0.005				
						E#	8791.930						
5	0	5 − 4 *, **	1	4		A	27485.52			−13.49	−0.85	27485.52	−0.02
						E	27499.01						
5	1	5 − 4 *, **	0	4		A	31266.31			19.05	0.57	31266.31	0.21
						E	31247.26						
5	2	3 − 4 *	3	2	6 − 5	A	5714.791			nm		5715.134	−0.033
					5 − 4	A	5716.026	−1.235	0.006				
					4 − 3	A	5714.537	0.254	0.000				
5	1	4 − 5	0	5	6 − 6	A	16646.770			10.975(0)	0.732	16647.207	−0.085
						E	16635.795						
					5 − 5	A	16648.352	−1.582	−0.003				
						E	16637.377						
					4 − 4	A	16646.440	0.330	−0.007				
						E	16635.464						
5	2	3 − 5	1	4		A	14802.475			17.540	0.389	14802.475	0.014
						E	14784.935						
6	0	6 − 5 *, **	1	5		A	33652.53			−8.31	−0.60	33652.53	0.19
						E	33660.84						
6	1	6 − 5 *, **	0	5		A	35952.45			15.00	1.05	35952.45	−0.24
						E	35937.45						

Table 2a (continued)

J'	K_-'	$K_+'-J''$	K_-''	K_+''	$F'-F''$	Γ	ν_{exp}	$\Delta\nu_{hfsA}$	$\delta_{calc-exp}$	$\Delta\nu_{AE}$ / $\Delta\nu_{AE\#}$	$\delta_{calc-exp}$	$\overline{\nu_{0A}}$	$\delta_{calc-exp}$
6	2	4 - 5	3	3	7 - 6	A	14435.309			-560.795(28)	0.512	14435.625	-0.053
						E	14996.120						
					6 - 5	A	14436.430	-1.121	-0.007				
						E	14997.186						
					5 - 4	A	14435.108	0.201	-0.018				
						E	14995.926						
6	2	5 - 5	3	2	7 - 6	A	6794.931			357.393(10)	0.038	6794.891	0.028
		*				E	6437.529						
					6 - 5	A	6794.789	0.142	-0.003				
						E	6437.406						
					5 - 4	A	6794.983	-0.052	0.017				
					6 - 6	A	6795.099	-0.168	-0.028				
6	1	5 - 6	0	6		A	21667.72			11.40	0.89	21667.72	-0.07
		*, **				E	21656.32						
6	2	4 - 6	1	5	7 - 7	A	15758.505			23.206(3)	0.522	15758.604	-0.010
						E	15735.304						
					6 - 6	A	15758.855	-0.350	0.001				
						E	15735.647						
					5 - 5	A	15758.443	0.062	-0.003				
						E	15735.235						
6	3	3 - 6	2	4		A	25310.02			-150.80	0.67	25310.02	-0.25
		*, **				E	25460.82						
6	5	2 - 7	4	3	7 - 8	A	7394.864			nm		7394.679	0.028
		*			6 - 7	A	7394.206	0.658	-0.001				
					5 - 6	A	7394.981	-0.117	0.014				
7	2	6 - 6	3	3	8 - 7	A	11141.744			194.931(30)	0.668	11141.620	0.033
		*				E	10946.797						
					7 - 6	A	11141.275	0.469	0.011				
						E	10946.386						
					6 - 5	A	11141.855	-0.111	0.026				
						E	10946.897						
7	2	5 - 7	1	6	8 - 8	A	17861.881			18.741(1)	0.790	17862.062	-0.045
						E	17843.139						
7	2	5 - 7	1	6	7 - 7	A	17862.525	-0.644	-0.007				
						E	17843.785						
					6 - 6	A	17861.766	0.115	-0.021				
						E	17843.024						
7	3	4 - 7	2	5		A	23703.90			-26.60	0.35	23703.90	0.05
		*, **				E	23730.50						
7	6	1 - 8	5	4	8 - 9	A	12910.079			nm		12909.931	-0.030
		*			7 - 8	A	12909.520	0.559	0.030				
					6 - 7	A	12910.206	-0.127	0.045				
7	6	2 - 8	5	3	8 - 9	A	12897.227			362.730(7)	0.403	12897.079	-0.029
						E#	12534.493						
					7 - 8	A	12896.670	0.557	0.035				
						E#	12533.933						
					6 - 7	A	12897.350	-0.123	0.040				
						E#	12534.630						
8	2	7 - 7	3	4	9 - 8	A	14256.702			66.736(16)	0.985	14256.470	0.060
						E	14189.961						
					8 - 7	A	14255.887	0.815	0.004				
						E	14189.172						
					7 - 6	A	14256.838	-0.136	0.017				
						E	14190.085						
8	3	6 - 7	4	3	9 - 8 }	A	10367.820			613.660(12)	-0.460	10367.891	-0.052
		*			7 - 6	E	9754.148						
					8 - 7	A	10368.028	-0.208	0.012				
						E	9754.380						
8	1	7 - 8	0	8		A	33288.37			24.20	0.38	33288.37	0.18
		*, **				E	33264.17						
8	2	6 - 8	1	7		A	21229.35			10.36	1.04	21229.35	-0.07
		*, **				E	21218.99						
8	3	5 - 8	2	6		A	22578.29			28.31	0.33	22578.29	-0.06
		*, **				E	22549.98						

Table 2a (continued)

J'	K_-'	$K_+'-J''$	K_-''	K_+''	$F'-F''$	Γ	ν_{exp}	$\Delta\nu_{hfsA}$	$\delta_{calc-exp}$	$\Delta\nu_{AE}$ / $\Delta\nu_{AE\#}$	$\delta_{calc-exp}$	$\overline{\nu_{0A}}$	$\delta_{calc-exp}$
8	6	2 - 9	5	5	9 - 10	A	6140.678			72.082(2)	0.064	6140.543	-0.007
		*				E#	6068.597						
					8 - 9	A	6140.209	0.469	0.005				
						E#	6068.124						
					7 - 8	A	6140.748	-0.070	0.015				
						E#	6068.668						
8	6	3 - 9	5	4	9 - 10	A	6096.363			351.217(1)	0.435	6096.225	-0.010
		*				E#	5745.147						
					8 - 9	A	6095.885	0.478	0.006				
						E#	5744.669						
					7 - 8	A	6096.433	-0.070	0.014				
						E#	5745.214						
9	2	8 - 8	3	5	10 - 9	A	15799.059			11.070(4)	1.094	15798.726	0.097
						E	15787.989						
					9 - 8	A	15797.918	1.141	0.006				
						E	15786.854						
					8 - 7	A	15799.219	-0.160	0.016				
						E	15788.144						
9	4	5 - 8	5	4	10 - 9	A	6949.406			nm		6949.560	-0.072
		*			9 - 8	A	6949.935	-0.529	-0.005				
					8 - 7	A	6949.334	0.072	-0.015				
9	4	6 - 8	5	3	10 - 9	A	6069.602			nm		6069.712	-0.068
		*			9 - 8	A	6069.977	-0.375	-0.003				
					8 - 7	A	6069.552	0.050	-0.010				
9	2	7 - 9	1	8		A	25826.40			2.20	1.40	25826.40	0.05
		*, **				E	25824.20						
9	3	6 - 9	2	7		A	22347.75			40.64	1.28	22347.75	-0.14
		*, **				E	22307.11						
9	4	5 - 9	3	6		A	35719.24			-218.21	0.09	35719.24	-0.11
		*, **				E	35937.45						
10	2	8 - 10	1	9			31423.00			nm		31423.00	0.03
		*, **											
10	3	7 - 10	2	8		A	23321.59			34.10	1.48	23321.59	-0.08
		*, **				E	23287.49						
10	4	6 - 10	3	7		A	33393.47			-60.89	0.38	33393.47	-0.09
		*, **				E	33454.36						
11	5	6 - 10	6	5	12 - 11 }	A	8022.210			nm		8022.342	-0.068
		*			10 - 9								
					11 - 10	A	8022.607	-0.397	-0.017				
11	3	8 - 11	2	9		A	25691.73			18.37	1.81	25691.73	-0.08
		*, **				E	25673.36						
11	4	7 - 11	3	8		A	31253.06			31.90	0.69	31253.06	0.15
		*, **				E	31221.16						
12	3	9 - 12	2	10		A	29516.90			0.90	1.16	29516.90	0.02
		*, **				E	29516.00						
13	6	7 - 12	7	6	14 - 13 }	A	9278.201			nm		9278.311	0.034
		*			12 - 11								
					13 - 12	A	9278.530	-0.329	-0.001				
13	3	10 - 13	2	11		A	34676.32			-14.99	1.86	34676.32	-0.07
		*, **				E	34691.31						
13	4	9 - 13	3	10		A	29476.74			61.41	1.27	29476.74	0.14
		*, **				E	29415.33						
14	4	10 - 14	3	11		A	30593.44			40.68	1.76	30593.44	0.16
		*, **				E	30552.76						
15	5	10 - 15	4	11		A	38311.79			84.88	0.47	38311.79	-0.17
		*, **				E	38226.91						
16	5	11 - 16	4	12		A	36653.85			96.82	1.33	36653.85	0.20
		*, **				E	36557.03						
17	5	12 - 17	4	13		A	36350.82			77.44	1.74	36350.82	-0.10
		*, **				E	36273.38						

Table 2b. Measured transitions of 4-methyl oxazole.

J'	K'_-	K'_+	$-J''$	K''_-	K''_+	$F'-F''$	Γ	ν_{exp}	$\Delta\nu_{hfs\,A}$	$\delta_{calc-exp}$	$\Delta\nu_{AE}$ $\Delta\nu_{AE\,\#}$	$\delta_{calc-exp}$	$\overline{\nu_{0A}}$	$\delta_{calc-exp}$
1	1	1	− 0	0	0	2 − 1	A	11837.160			2.540(4)	0.009	11837.015	−0.019
							E	11834.625						
						1 − 1	A	11836.266	0.894	0.002				
							E	11833.726						
						0 − 1	A	11838.516	−1.356	0.011				
							E	11835.971						
2	1	2	− 1	0	1	3 − 2	A	17026.657			2.251(3)	0.013	17026.460	−0.013
							E	17024.405						
						2 − 1	A	17025.710	0.947	−0.001				
							E	17023.460						
						1 − 1	A	17026.868	−0.211	0.007				
							E	17024.621						
						1 − 0	A	17027.378	−0.721	0.000				
							E	17025.122						
2	2	0	− 1	1	1		A	31362.06			−8.04	0.68	31362.06	−0.08
			*, **				E	31370.10						
2	2	1	− 1	1	0		A	30321.41			19.38	0.61	30321.41	0.04
			*, **				E	30302.03						
2	2	0	− 2	1	1	3 − 3	A	17243.714			−6.817(12)	0.019	17243.473	−0.027
							E	17250.527						
						2 − 2	A	17242.652	1.062	−0.009				
							E	17249.456						
						1 − 1	A	17244.288	−0.574	−0.011				
							E	17251.121						
3	0	3	− 2	1	2	4 − 3	A	13075.794			−2.088(0)	0.003	13075.931	−0.013
							E	13077.881						
						3 − 2	A	13076.433	−0.639	−0.005				
							E	13078.521						
						2 − 1	A	13075.412	0.382	−0.005				
							E	13077.500						
3	1	3	− 2	0	2		A	21791.40			2.00	0.18	21791.40	−0.01
			*, **				E	21789.40						
3	1	2	− 3	0	3	4 − 4	A	9433.829			1.898(2)	0.013	9434.102	−0.070
							E	9431.929						
						3 − 3	A	9434.932	−1.103	0.001				
							E	9433.033						
						2 − 2	A	9433.434	0.395	−0.009				
							E	9431.539						
3	2	1	− 3	1	2	4 − 4	A	16325.254			3.216(1)	0.022	16325.084	−0.022
							E	16322.038						
						3 − 3	A	16324.574	0.680	0.003				
							E	16321.356						
						2 − 2	A	16325.493	−0.239	0.000				
							E	16322.278						
3	3	0	− 4	2	3	5 − 4	A	6555.478			−45.806(3)	0.024	6555.406	−0.042
			*				E	6601.282						
						4 − 3	A	6555.170	0.308	−0.005				
							E	6600.980						
3	3	0	− 4	2	3	3 − 2	A	6555.598	−0.120	0.020				
			*				E	6601.403						
3	3	1	− 4	2	2	5 − 4	A	5045.170			nm		5044.944	−0.010
			*			4 − 3	A	5044.308	0.862	0.005				
						3 − 2	A	5045.414	−0.244	−0.002				
4	0	4	− 3	1	3		A	19681.34			−1.50	−0.24	19681.34	0.02
			*, **				E	19682.84						
4	1	4	− 3	0	3		A	26269.43			2.00	0.07	26269.43	−0.23
			*, **				E	26267.43						
4	1	3	− 4	0	4	5 − 5	A	12052.239			1.732(4)	0.012	12052.589	−0.127
							E	12050.512						
						4 − 4	A	12053.538	−1.299	0.001				
							E	12051.806						
						3 − 3	A	12051.915	0.324	0.010				
							E	12050.178						

Table 2b (continued)

J'	K'_-	K'_+	$-J''$	K''_-	K''_+	$F'-F''$	Γ	ν_{exp}	$\Delta\nu_{hfs\,A}$	$\delta_{calc-exp}$	$\Delta\nu_{AE}$ $\Delta\nu_{AE\,\#}$	$\delta_{calc-exp}$	$\overline{\nu_{0A}}$	$\delta_{calc-exp}$
4	2	2	− 4	1	3	5 − 5	A	15591.652			4.803(1)	0.025	15591.559	−0.022
							E	15586.850						
						4 − 4	A	15591.295	0.357	0.000				
							E	15586.491						
						3 − 3	A	15591.750	−0.098	0.006				
							E	15586.948						
4	2	3	− 4	1	4		A	23385.11			7.12	0.12	23385.11	0.27
			*, **				E	23377.99						
5	0	5	− 4	0	4		A	28822.85			nm		28822.85	0.00
			*, **											
5	1	5	− 4	0	4		A	30649.77			1.79	0.09	30649.77	−0.05
			*, **				E	30647.98						
5	1	4	− 5	0	5	6 − 6	A	15644.177			1.513(3)	0.021	15644.577	−0.201
							E	15642.666						
						5 − 5	A	15645.621	−1.444	0.005				
							E	15644.104						
						4 − 4	A	15643.879	0.298	−0.005				
							E	15642.368						
5	2	3	− 5	1	4	6 − 6	A	15359.346			4.786(1)	0.021	15359.326	−0.033
			*			4 − 4	E	15354.561						
						5 − 5	A	15359.289	0.057	−0.007				
							E	15354.503						
5	4	1	− 6	3	4	7 − 6	A	5896.173			−65.987(2)	0.028	5896.085	−0.023
			*			5 − 4	E	5962.162						
						6 − 5	A	5895.891	0.282	0.038				
							E	5961.876						
5	4	2	− 6	3	3	7 − 6	A	5290.372			95.328(3)	0.038	5290.249	−0.034
			*				E	5195.044						
						6 − 5	A	5289.914	0.458	0.010				
							E	5194.589						
						5 − 4	A	5290.473	−0.101	0.020				
							E	5195.141						
6	0	6	− 5	0	5		A	33976.53			nm		33976.53	−0.08
			*, **											
6	0	6	− 5	1	5		A	32149.60			−0.78	−0.11	32149.60	−0.02
			*, **				E	32150.38						
6	1	5	− 5	2	4		A	26433.35			−5.92	−0.19	26433.35	−0.12
			*, **				E	26439.27						
6	1	6	− 5	0	5		A	35107.97			1.56	0.03	35107.97	0.10
			*, **				E	35106.41						
6	1	6	− 5	1	5		A	33281.29			nm		33281.29	−0.09
			*, **											
6	1	5	− 6	0	6		A	20161.98			1.37	0.07	20161.98	0.21
			*, **				E	20160.61						
6	2	4	− 6	1	5	7 − 7	A	15893.663			4.203(2)	0.025	15893.726	−0.060
							E	15889.458						
						6 − 6	A	15893.900	−0.237	−0.004				
							E	15889.697						
						5 − 5	A	15893.609	0.054	−0.013				
							E	15889.409						
6	2	5	− 6	1	6		A	28872.28			5.81	0.64	28872.28	−0.13
			*, **				E	28866.47						
6	3	3	− 6	2	4		A	27176.21			5.89	−0.18	27176.21	0.02
			*, **				E	27170.32						
6	5	2	− 7	4	3	7 − 8	A	11865.713			nm		11865.622	−0.062
			*			6 − 7	A	11865.384	0.329	0.012				
						5 − 6	A	11865.776	−0.063	0.011				
7	1	6	− 6	2	5		A	34469.46			−5.11	−0.22	34469.46	−0.08
			*, **				E	34474.57						

Table 2b (continued)

J'	K'_-	$K'_+ - J''$	K''_-	K''_+	$F' - F''$	Γ	ν_{exp}	$\Delta\nu_{hfsA}$	$\delta_{calc-exp}$	$\Delta\nu_{AE}$ $\Delta\nu_{AE\#}$	$\delta_{calc-exp}$	$\overline{\nu_{0A}}$	$\delta_{calc-exp}$
7	2	5 - 7	1	6	8 - 8	A	17393.382			3.329(2)	0.024	17393.523	-0.112
						E	17390.056						
					7 - 7	A	17393.875	-0.493	-0.005				
						E	17390.544						
					6 - 6	A	17393.301	0.081	-0.009				
						E	17389.972						
7	2	6 - 7	1	7		A	32330.42			6.12	0.28	32330.42	0.01
		*, **				E	32324.30						
7	3	4 - 7	2	5		A	25554.55			8.50	0.06	25554.55	-0.06
		*, **				E	25546.05						
7	3	5 - 7	2	6		A	33909.33			11.02	0.72	33909.33	0.14
		*, **				E	33898.31						
7	5	2 - 8	4	5	8 - 9	A	5503.661			-99.341(7)	0.052	5503.575	-0.036
		*			6 - 7	E	5602.995			159.215(16)	-0.081		
						E#	5344.462						
					7 - 8	A	5503.399	0.262	0.010				
						E	5602.746						
						E#	5344.169						
7	5	3 - 8	4	4	8 - 9	A	5292.953			136.475(37)	-0.076	5292.861	-0.040
		*			6 - 7	E	5156.441			-122.182(15)	0.158		
						E#	5415.120						
					7 - 8	A	5292.661	0.292	0.030				
						E	5156.223						
						E#	5414.858						
8	3	6 - 7	4	3	9 - 8	A	6423.063			35.490(1)	-0.052	6423.105	-0.022
		*			7 - 6	E	6387.573						
					8 - 7	A	6423.176	-0.113	0.024				
						E	6387.687						
8	2	6 - 8	1	7		A	19995.91			2.24	0.07	19995.91	0.14
		*, **				E	19993.67						
8	2	7 - 8	1	8		A	36197.76			6.22	0.25	36197.76	0.17
		*, **				E	36191.54						
8	3	5 - 8	2	6		A	24161.54			8.87	0.06	24161.54	-0.05
		*, **				E	24152.67						
8	3	6 - 8	2	7		A	35668.09			9.30	0.91	35668.09	-0.04
		*, **				E	35658.79						
8	6	3 - 9	5	4	9 - 10	A	11699.017			26.114(7)	0.052	11698.932	-0.077
		*			7 - 8	E#	11672.896						
					8 - 9	A	11698.759	0.258	0.008				
						E#	11672.652						
9	2	8 - 8	3	5	10 - 9	A	14701.586			-5.984(1)	-0.002	14701.309	0.122
						E	14707.569						
					9 - 8	A	14700.640	0.946	0.002				
						E	14706.625						
					8 - 7	A	14701.713	-0.127	0.010				
						E	14707.696						
9	3	6 - 8	4	5	10 - 9	A	17834.908			nm		17835.096	-0.096
		*			9 - 8	A	17835.536	-0.628	-0.010				
					8 - 7	A	17834.836	0.072	-0.005				
9	2	7 - 9	1	8		A	23748.69			1.05	0.21	23748.69	0.26
		*, **				E	23747.64						
9	3	6 - 9	2	7		A	23374.80			7.99	0.13	23374.80	0.07
		*, **				E	23366.81						
9	3	7 - 9	2	8		A	37935.42			8.60	0.73	37935.42	-0.03
		*, **				E	37926.82						
9	4	5 - 9	3	6		A	38696.11			5.85	0.22	38696.11	0.09
		*, **				E	38690.26						
9	6	3 - 10	5	6	10 - 11	A	5224.391			45.326(4)	0.023	5224.316	-0.047
		*			8 - 9	E#	5179.069						
					9 - 10	A	5224.165	0.226	0.000				
						E#	5178.836						

Table 2b (continued)

J'	K'_-	$K'_+ - J''$	K''_-	K''_+	$F' - F''$	Γ	ν_{exp}	$\Delta\nu_{hfsA}$	$\delta_{calc-exp}$	$\Delta\nu_{AE}$ $\Delta\nu_{AE\#}$	$\delta_{calc-exp}$	$\overline{\nu_{0A}}$	$\delta_{calc-exp}$
9	6	4 - 10	5	5	10 - 11	A	5156.447			-1.146(9)	0.073	5156.367	-0.052
		*			8 - 9	E#	5157.584						
9	6	4 - 10	5	5	9 - 10	A	5156.208	0.239	0.000				
		*				E#	5157.363						
10	2	9 - 9	3	6	11 - 10	A	15478.433			-4.887(9)	-0.009	15478.084	0.187
		*				E	15483.311						
					10 - 9	A	15477.232	1.201	-0.006				
						E	15482.127						
					9 - 8	A	15478.599	-0.166	0.035				
						E	nm						
10	3	8 - 9	4	5	11 - 10	A	17498.937			-2.255(1)	-0.004	17498.879	-0.088
		*			9 - 8	E	17501.191						
					10 - 9	A	17498.763	0.174	-0.002				
						E	17501.018						
10	4	7 - 9	5	4	11 - 10	A	7483.075			68.761(2)	-0.060	7483.138	-0.042
		*			9 - 8	E	7414.312						
					10 - 9	A	7483.260	-0.185	0.008				
						E	7414.501						
10	3	7 - 10	2	8		A	23513.56			6.57	0.06	23513.56	-0.102
		*, **				E	23506.99						
10	4	6 - 10	3	7		A	36566.07			11.70	0.12	36566.07	0.01
		*, **				E	36554.37						
10	7	3 - 11	6	6	11 - 12	A	11511.202			nm		11511.134	-0.104
		*			9 - 10	E	11714.411						
					10 - 11	A	11510.996	0.206	0.004				
						E	11714.323						
11	2	10 - 10	3	7	12 - 11	A	14602.927			-3.425(1)	-0.003	14602.506	0.321
						E	14606.351						
					11 - 10	A	14601.527	1.400	0.008				
						E	14604.953						
					10 - 9	A	14603.078	-0.151	0.013				
						E	14606.503						
11	4	7 - 10	5	6	12 - 11	A	16363.143			-87.633(2)	0.007	16363.263	-0.049
						E	16450.777						
					11 - 10	A	16363.544	-0.401	-0.003				
						E	16451.174						
					10 - 9	A	16363.100	0.043	-0.009				
						E	16450.736						
11	4	8 - 10	5	5	12 - 11	A	13922.511			48.960(2)	-0.048	13922.560	-0.104
		*			10 - 9	E	13873.549						
					11 - 10	A	13922.651	-0.140	0.014				
						E	13873.693						
11	3	8 - 11	2	9		A	24805.32			4.15	0.56	24805.32	-0.08
		*, **				E	24801.17						
11	4	7 - 11	3	8		A	34312.73			12.82	0.82	34312.73	-0.12
		*, **				E	34299.91						
12	5	8 - 11	6	5	13 - 12	A	8019.284			-348.778(14)	0.208	8019.351	-0.043
		*			11 - 10	E#	8368.048						
					12 - 11	A	8019.479	-0.195	0.011				
						E#	8368.271						
12	3	9 - 12	2	10		A	27384.79			2.40	0.19	27384.79	0.13
		*, **				E	27382.39						
12	4	8 - 12	3	9		A	32332.52			12.70	0.67	32332.52	-0.04
		*, **				E	32319.82						
13	5	8 - 12	6	7	14 - 13	A	15642.611			-131.020(1)	0.079	15642.698	-0.037
		*			12 - 11	E	15773.631						
					13 - 12	A	15642.875	-0.264	-0.003				
						E	15773.894						
13	5	9 - 12	6	6	14 - 13	A	14734.204			85.222(2)	-0.126	14734.261	-0.108
		*			12 - 11	E	14648.980						
					13 - 12	A	14734.373	-0.169	0.004				
						E	14649.153						

Table 2b (continued)

J'	K'_-	$K'_+ - J''$	K''_-	K''_+	$F' - F''$	Γ	ν_{exp}	$\Delta\nu_{hfs\,A}$	$\delta_{calc-exp}$	$\Delta\nu_{AE}$ $\Delta\nu_{AE\#}$	$\delta_{calc-exp}$	$\overline{\nu_{0A}}$	$\delta_{calc-exp}$
13	3	10 - 13	2	11		A	31275.45			0.41	0.12	31275.45	0.17
		*, **				E	31275.04						
13	4	9 - 13	3	10		A	31047.73			11.79	-0.04	31047.73	-0.05
		*, **				E	31035.94						
14	6	8 - 13	7	7	15 - 14	A	8477.245			45.752(5)	-0.075	8477.311	-0.001
		*			13 - 12	E#	8431.489						
					14 - 13	A	8477.438	-0.193	0.008				
						E#	8431.691						
14	6	9 - 13	7	6	15 - 14	A	8341.043			-97.459(17)	0.106	8341.102	-0.025
		*			13 - 12	E#	8438.485						
					14 - 13	A	8341.217	-0.174	0.006				
						E#	8438.693						
14	3	11 - 14	2	12		A	36352.24			-1.12	0.04	36352.24	0.24
		*, **				E	36353.36						
14	4	10 - 14	3	11		A	30818.67			8.96	0.25	30818.67	0.20
		*, **				E	30809.71						
15	6	9 - 14	7	8	16 - 15	A	15452.681			190.417(6)	-0.181	15452.747	-0.039
		*			14 - 13	E#	15262.270						
					15 - 14	A	15452.878	-0.197	0.004				
						E#	15262.456						
15	6	10 - 14	7	7	16 - 15	A	15144.229			-242.653(7)	0.129	15144.295	-0.100
		*			14 - 13	E#	15386.875						
					15 - 14	A	15144.414	-0.185	0.024				
						E#	15387.073						
15	4	11 - 15	3	12		A	31901.12			5.70	0.40	31901.12	0.13
		*, **				E	31895.42						
16	4	12 - 16	3	13		A	34434.88			2.40	0.34	34434.88	0.04
		*, **				E	34432.48						
17	7	10 - 16	8	9	18 - 17	A	15504.059			nm		15504.120	-0.032
		*			16 - 15								
					17 - 16	A	15504.232	-0.173	0.017				
17	7	11 - 16	8	8	18 - 17	A	15405.143			nm		15405.206	-0.064
		*			16 - 15								
					17 - 16	A	15405.317	-0.174	0.028				
17	5	12 - 17	4	13		A	38508.14			14.80	0.87	38508.14	-0.24
		*, **				E	38493.34						
18	3	16 - 17	4	13	19 - 18	A	12857.062			4.713(2)	-0.010	12856.620	0.065
						E	12852.352						
					18 - 17	A	12855.630	1.432	0.012				
						E	12850.916						
					17 - 16	A	12857.174	-0.112	0.028				
						E	12852.460						
18	8	11 - 17	9	8	19 - 18	A	8816.634			241.463(6)	-0.851	8816.687	0.073
		*, **			17 - 16	E	8575.166						
					18 - 17	A	8816.785	-0.151	0.019				
						E	8575.328						
18	5	13 - 18	4	14		A	37921.24			11.49	0.51	37921.24	-0.01
		*, **				E	37909.75						
19	8	11 - 18	9	10	20 - 19	A	15652.157			-27.525(2)	0.013	15652.213	0.010
		*			18 - 17	E#	15679.683						
					19 - 18	A	15652.314	-0.157	0.024				
						E#	15679.837						
19	8	12 - 18	9	9	20 - 19	A	15621.646			-35.469(1)	-0.032	15621.701	-0.006
		*			18 - 17	E#	15657.115						
					19 - 18	A	15621.800	-0.154	0.023				
						E#	15657.268						
19	5	14 - 19	4	15		A	38784.08			7.52	0.05	38784.08	-0.06
		*, **				E	38776.56						

Table 2c. Measured transitions of 5-methyl oxazole.

J'	K'_-	$K'_+ - J''$	K''_-	K''_+	$F' - F''$	Γ	ν_{exp}	$\Delta\nu_{hfs\,A}$	$\delta_{calc-exp}$	$\Delta\nu_{AE}$ $\Delta\nu_{AE\#}$	$\delta_{calc-exp}$	$\overline{\nu_{0A}}$	$\delta_{calc-exp}$
2	0	2 - 1	0	1	3 - 2	A	12303.308			0.024	0.000	12303.248	-0.083
		*, **				E	12303.284						
2	1	1 - 1	1	0	3 - 2	A	13365.081			0.098(7)	0.002	13364.976	-0.080
						E	13364.980						
					2 - 1	A	13364.428	0.653	0.007				
						E	13364.323						
					1 - 0	A	13366.133	-1.052	0.001				
						E	13366.045						
2	1	2 - 1	1	1	3 - 2	A	11460.138			-0.102(1)	0.008	11459.977	-0.084
						E	11460.239						
					2 - 1	A	11459.424	0.714	0.002				
						E	11459.526						
3	0	3 - 2	0	2		A	18190.89			nm		18190.89	-0.02
		*, **											
3	1	2 - 2	1	1		A	19974.63			nm		19974.63	0.06
		*, **											
3	1	3 - 2	1	2	4 - 3		17125.287			0.000	-0.010	17125.199	-0.113
		**			3 - 2		17125.048	0.239	-0.008				
					2 - 1		17125.191	0.096	-0.017				
3	2	1 - 2	2	0		A	19046.20			3.08	0.55	19046.20	0.08
		*, **				E	19043.12						
3	2	2 - 2	2	1		A	18618.56			-3.39	-0.32	18618.56	-0.01
		*, **				E	18621.95						
3	1	2 - 3	0	3	4 - 4	A	9523.320			1.139(5)	-0.008	9523.505	-0.004
						E	9522.187						
					3 - 3	A	9524.060	-0.740	-0.005				
						E	9522.922						
					2 - 2	A	9523.059	0.261	0.000				
						E	9521.914						
3	2	1 - 3	1	2	4 - 4	A	16357.123			2.621(7)	-0.002	16357.186	-0.008
						E	16354.492						
					3 - 3	A	16357.404	-0.281	-0.002				
						E	16354.791						
					2 - 2	A	16357.002	0.121	-0.022				
						E	16354.383						
4	0	4 - 3	0	3		A	23809.23			nm		23809.23	0.00
		*, **											
4	1	3 - 3	1	2		A	26485.98			nm		26485.98	0.08
		*, **											
4	1	4 - 3	1	3		A	22722.90			nm		22722.90	0.14
		*, **											
4	2	2 - 3	2	1		A	25754.52			0.42	0.08	25754.52	0.08
		*, **				E	25754.10						
4	2	3 - 3	2	2		A	24739.47			-0.47	-0.16	24739.47	0.03
		*, **				E	24739.94						
4	3	1 - 3	3	0		A	25068.30			14.30	-0.19	25068.30	0.05
		*, **				E	25054.00						
4	3	2 - 3	3	1		A	25021.54			-14.01	-0.18	25021.54	-0.13
		*, **				E	25035.55						
4	1	3 - 4	0	4	5 - 5	A	12200.140			1.027(4)	-0.002	12200.341	-0.005
						E	12199.118						
					4 - 4	A	12200.894	-0.754	0.000				
						E	12199.865						
					3 - 3	A	12199.945	0.195	-0.001				
						E	12198.915						
4	1	3 - 4	1	4	5 - 5		9469.879					9470.112	0.014
					4 - 4		9470.759	-0.880	0.001				
					3 - 3		9469.646	0.233	-0.007				

Table 2c (continued)

J'	K'_-	$K'_+ - J''$	K''_-	K''_+	$F'-F''$	Γ	ν_{exp}	$\Delta\nu_{hfsA}$	$\delta_{calc-exp}$	$\Delta\nu_{AE}$ / $\Delta\nu_{AE\#}$	$\delta_{calc-exp}$	$\overline{\nu_{0A}}$	$\delta_{calc-exp}$
4	2	2 - 4	1	3	5 - 5	A	15625.680			3.045(3)	0.005	15625.726	-0.006
						E	15622.635						
					4 - 4	A	15625.867	-0.187	0.002				
						E	15622.818						
					3 - 3	A	15625.619	0.061	-0.014				
						E	15622.578						
5	0	5 - 4	0	4		A	29178.07			nm		29178.07	0.091
		*,**											
5	1	4 - 4	1	3		A	32848.06			nm		32848.06	0.052
		*,**											
5	1	5 - 4	1	4		A	28246.87			nm		28246.87	0.093
		*,**											
5	2	3 - 4	2	2		A	32637.64			nm		32637.64	-0.103
		*,**											
5	2	4 - 4	2	3		A	30788.48			nm		30788.48	-0.033
		*,**											
5	3	2 - 4	3	1		A	31491.90			11.03	0.05	31491.90	-0.045
		*,**				E	31480.87						
5	3	3 - 4	3	2		A	31330.67			-11.08	-0.13	31330.67	-0.055
		*,**				E	31341.75						
5	1	4 - 5	0	5	6 - 6	A	15870.093			0.893(4)	0.006	15870.306	-0.020
						E	15869.200						
					5 - 5	A	15870.872	-0.779	0.001				
						E	15869.973						
					4 - 4	A	15869.923	0.170	-0.012				
						E	15869.035						
5	1	4 - 5	1	5	6 - 6	A	14071.047			0.090(3)	-0.006	14071.285	-0.011
						E	14070.958						
					5 - 5	A	14071.918	-0.871	0.000				
						E	14071.824						
5	1	4 - 5	1	5	4 - 4	A	14070.856	0.191	-0.014				
						E	14070.770						
5	2	3 - 5	1	4	6 - 6	A	15415.101			2.891(2)	-0.001	15415.154	-0.009
						E	15412.210						
					5 - 5	A	15415.300	-0.199	-0.001				
						E	15412.412						
					4 - 4	A	15415.055	0.046	-0.005				
						E	15412.161						
6	0	6 - 5	0	5		A	34391.26			nm		34391.26	0.09
		*,**											
6	1	5 - 5	1	4		A	38999.14			nm		38999.14	-0.06
		*,**											
6	1	6 - 5	1	5		A	33699.49			nm		33699.49	0.02
		*,**											
6	2	4 - 5	2	3		A	39579.19			nm		39579.19	-0.04
		*,**											
6	2	5 - 5	2	4		A	36750.11			nm		36750.11	-0.08
		*,**											
6	3	3 - 5	3	2		A	38057.60			3.33	-0.09	38057.60	-0.03
		*,**				E	38054.27						
6	2	4 - 6	1	5	7 - 7	A	15995.151			2.492(0)	0.001	15995.221	-0.005
						E	15992.659						
					6 - 6	A	15995.409	-0.258	0.000				
						E	15992.916						
					5 - 5	A	15995.097	0.054	-0.010				
						E	15992.605						
7	2	5 - 7	1	6	8 - 8	A	17567.077			1.949(3)	0.002	17567.166	-0.007
						E	17565.125						
					7 - 7	A	17567.399	-0.322	-0.008				
						E	17565.454						
					6 - 6	A	17567.015	0.062	-0.014				
						E	17565.065						

Table 2c (continued)

J'	K'_-	$K'_+ - J''$	K''_-	K''_+	$F'-F''$	Γ	ν_{exp}	$\Delta\nu_{hfsA}$	$\delta_{calc-exp}$	$\Delta\nu_{AE}$ / $\Delta\nu_{AE\#}$	$\delta_{calc-exp}$	$\overline{\nu_{0A}}$	$\delta_{calc-exp}$
7	2	5 - 7	2	6	8 - 8	A	10067.674			-1.199(7)	0.000	10067.817	0.029
						E	10068.869						
					7 - 7	A	10068.172	-0.498	-0.010				
						E	10069.381						
					6 - 6	A	10067.594	0.080	-0.007				
						E	10068.787						
8	2	6 - 8	2	7	9 - 9	A	14853.522			-1.386(2)	-0.001	14853.680	0.003
						E	14854.905						
					8 - 8	A	14854.070	-0.548	-0.005				
						E	14855.457						
					7 - 7	A	14853.440	0.082	-0.013				
						E	14854.828						
8	3	5 - 8	2	6		A	24169.97			5.27	0.15	24169.97	0.01
		*,**				E	24164.70						
9	3	6 - 9	2	7		A	23427.80			4.90	-0.10	23427.80	-0.01
		*,**				E	23422.90						
10	3	7 - 10	2	8		A	23647.70			3.90	-0.05	23647.70	0.03
		*,**				E	23643.80						
10	3	7 - 10	3	8	11 - 11	A	9260.589			-2.514(1)	-0.001	9260.689	0.052
						E	9263.103						
					10 - 10	A	9260.926	-0.337	-0.001				
						E	9263.441						
					9 - 9	A	9260.549	0.040	-0.006				
						E	9263.062						
11	3	8 - 11	3	9	12 - 12	A	13969.127			-3.084(0)	0.000	13969.244	0.012
						E	13972.211						
					11 - 11	A	13969.521	-0.394	0.000				
						E	13972.605						
11	3	8 - 11	3	9	10 - 10	A	13969.082	0.045	-0.009				
						E	13972.165						
12	3	9 - 12	2	10		A	27784.88			1.34	0.08	27784.88	-0.07
		*,**				E	27783.54						
13	3	10 - 13	2	11		A	31843.53			nm		31843.53	0.07
		*,**											
13	4	9 - 13	3	10		A	31073.55			7.04	-0.19	31073.55	-0.01
		*,**				E	31066.51						
14	4	10 - 14	3	11		A	30969.87			5.22	0.04	30969.87	-0.04
		*,**				E	30964.65						
14	4	10 - 14	4	11	15 - 15	A	12075.825			-4.571(1)	0.002	12075.911	0.021
						E	12080.395						
					14 - 14	A	12076.110	-0.285	-0.002				
						E	12080.682						
					13 - 13	A	12075.797	0.028	-0.007				
						E	12080.369						
15	4	11 - 15	3	12		A	32222.95			3.25	0.13	32222.95	0.022
		*,**				E	32219.70						
15	4	11 - 15	4	12	16 - 16	A	17575.961			-5.537(6)	-0.001	17576.066	-0.087
						E	17581.502						
					15 - 15	A	17576.303	-0.342	0.007				
						E	17581.832						
					14 - 14	A	17575.932	0.029	-0.007				
						E	17581.474						
16	4	12 - 16	3	13		A	34962.97			1.20	0.19	34962.97	0.09
		*,**				E	34961.77						
17	5	12 - 17	4	13		A	34484.09			8.21	0.81	34484.09	0.05
		*,**				E	38475.88						
18	5	13 - 18	4	14		A	38072.85			6.81	-0.07	38072.85	-0.07
		*,**				E	38066.04						

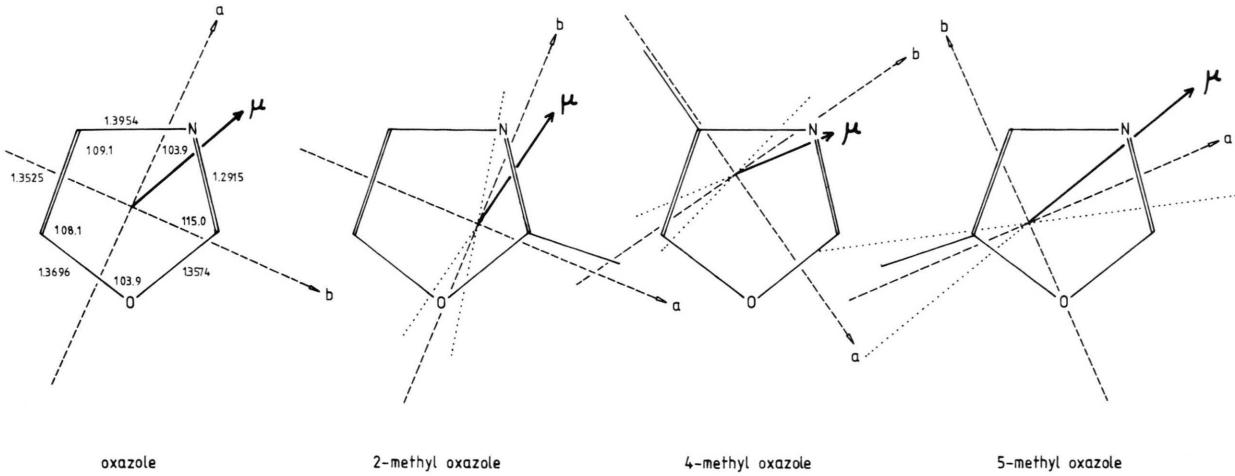

Fig. 2. Possible lines of action of the total dipole moment and the most probable of the four possible alignments. – For oxazole the direction of the total dipole moment has been determined by isotopic substitution [2]. – – – – Principal inertia axes *a* and *b*; · · · · · · possible lines of action of the total dipole moment; μ: most probable alignment of the total moment.

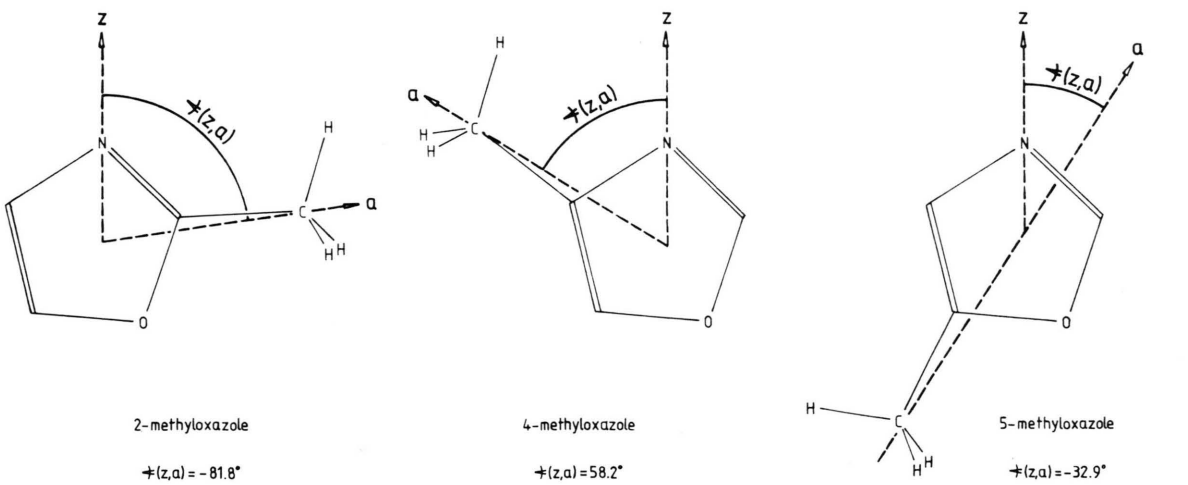

Fig. 3. Variation of the angle between the *z*-axis of the principal quadrupole coupling tensor at the ^{14}N-atom and the principal inertia axis *a*, $\sphericalangle(z, a)$, with the three possible positions of the methyl group at the oxazole ring.

against the square of the applied field were obtained for nearly all the relevant M-states, with $\Delta\nu$ up to some 10 MHz. The dipole moment components obtained by the usual methods of analysis are shown in Table 1.

These components conform with the observations, above, of the predominant types of line in each spectrum. The total moments of 2-methyl and 4-methyl oxazoles are somewhat smaller than that of oxazole [2] (1.50 D), while the moment of 5-methyl oxazole is noticeably greater than that figure. This least finding resembles observations made for 3-methyl furan [10] and 3-methyl thiophen [11], the moments for which exceed those of furan and thiophen, respectively, by some 0.4 D. Since the *a*-axes in all the methyl oxazoles must lie close to the lines of the methyl C-ring bond (see discussion below and Figs. 2 and 3), the results in Table 1 define, for each molecule, two possible lines of action of the total moment in the *a*/*b* axis frame. The most probable lines of action do not differ greatly, with respect to the ring atoms, from the line of the moment in oxazole itself [2] (see Figure 2).

Analysis

The experimental line frequencies were evaluated by a nuclear quadrupole hyperfine structure, a centrifugal distortion, and an internal rotation analysis separately, presupposing that the three perturbations of the rigid rotor hamiltonian can be treated independently, an assumption which later proved to be justified by the standard deviation of the respective fit. The centrifugal distortion analysis was performed only for the torsional A species lines because of their pseudo-rigid rotor behaviour, the prime object being an extrapolation of the microwave spectra from lower to higher J quantum numbers and only in the second place the determination of centrifugal distortion parameters. As, in accordance with our assumption above, the A and E species ^{14}N-hfs patterns do not differ significantly, the ^{14}N-hfs analysis was also done for the A lines only. The E species components could thus easily be identified by superimposing their ^{14}N-hfs patterns and those of the corresponding A lines. By a centrifugal distortion analysis of all line centre frequencies and the consistency of ^{14}N-hfs and methyl internal rotation analyses with increasing J value, the assignment of the rotational spectra could be confirmed.

For the nuclear quadrupole hfs analysis the possible set of lines was limited to completely split low J A-type transitions measured with MWFT technique. The quadrupole coupling constants $\chi_+ = \chi_{bb} + \chi_{cc}$ and $\chi_- = \chi_{bb} - \chi_{cc}$ were fitted to ^{14}N-hfs splittings relative to the most intense component $\Delta\nu_{\mathrm{hfs\,A}}$ with a first order perturbation treatment[1] which appeared to be adequate. To get information about the off-diagonal quadrupole coupling tensor element χ_{ab}, one has to take into consideration the structures of isotopic species with a rotated inertial axes system relative to the parent molecule beside their respective quadrupole coupling constants.

With the quadrupole coupling constants χ_+ and χ_- as results from the ^{14}N-hfs analysis we then calculated the frequency shifts from the rigid rotor position, corrected the single experimental hfs components of one rotational line by these shifts, and finally as arithmetic mean values we got hypothetical A species line centre frequencies $\overline{\nu_{0\mathrm{A}}}$ as input data for the centrifugal distortion analysis. A fourth order centrifugal distortion analysis according to Watson's S-reduction [12, 13] with the hamiltonian operator already cited as equation (1) in [4] was carried out for all transitions measured in Bangor and Kiel[2].

^{14}N-hfs and centrifugal distortion analyses were performed in an iterative manner, until χ_+ and χ_- on the one hand and the rotational and centrifugal distortion constants on the other hand had converged to their final values, The results of both analyses are contained in Tables 3a–c.

As A-E splittings $\Delta\nu_{\mathrm{AE}}$ for an IAM internal rotation analysis we took the arithmetic mean of the methyl torsional splittings of the single hfs components for every rotational line measured with the MWFT spectrometer in Kiel. We used the program written by Woods [14, 15], modified by H. Lutz, E. Fliege, and G. Bestmann[3]. With the additional measurements mentioned above and only needed for this purpose, we succeeded in fitting all three internal rotation parameters, namely $w_1(\mathrm{s})$, first Fourier coefficient in the expansion of the eigenvalues of the Mathieu differential equation for the torsional ground state $v = 0$, I_α, moment of inertia of the methyl group, and $\measuredangle(a, i)$, angle between the principal inertia axis a and the internal rotation axis i of the methyl group, to the experimental data of all three methyl oxazoles. This angle $\measuredangle(a, i)$, which we need for a comparison of electric field gradient tensors at ^{14}N in the related molecules (see Section "Discussion"), could in the case of 2- and 4-methyl oxazole only be obtained after including the additional measurements. The results of the IAM torsional analysis are summarized in Tables 4a–c together with some derived data.

Discussion

To study the influence of methyl substitution on the electric field gradient tensor at nitrogen-^{14}N, we tried to optimize the structure of the respective methyl derivative, took over the principal ^{14}N quadrupole coupling tensor from oxazole [2], and calculated the projections χ_{aa} and χ_{bb} of the principal tensor elements χ_{xx} and χ_{zz} (oxazole) on the principal intertia axes a and b of the respective methyl compound.

[1] Programs HT1NQ, QUAD, and DH14KS.

[2] Program ZFAP4 by V. Typke (1982).

[3] Programs IAMCAL, IAMFIT, and IAMMOD.

Table 3. Rotational [MHz], centrifugal distortion [kHz] and nitrogen-14 quadrupole coupling [MHz] constants of 2-, 4- and 5-methyloxazole. A, B, C: rotational constants, D_J, D_{JK}, D_K, d_1, d_2: fourth order centrifugal distortion constants according to Watson's S-reduction, N: number of rotational lines used for centrifugal distortion and ^{14}N quadrupole hfs analysis respectively, σ: standard deviation of the fit [kHz], χ_+, χ_-: quadrupole coupling constants ($\chi_+ = \chi_{bb} + \chi_{cc}$ and $\chi_- = \chi_{bb} - \chi_{cc}$), N_{spl}: number of splittings used for ^{14}N-hfs analysis, $\overline{\Delta\nu_{hfs}}$: mean experimental hfs splitting [kHz]; fixed values in square brackets, standard errors in units of the last digit in round brackets.

Table 3a. 2-Methyl oxazole.

		Correlation matrix						
A	9128.3291(92)	1.00						
B	3717.0007(39)	0.72	1.00					
C	2684.1280(35)	0.68	0.69	1.00				
D_J	0.319 (23)	0.51	0.53	0.68	1.00			
D_{JK}	1.844 (39)	0.54	0.42	0.22	0.02	1.00		
D_K	16.92 (16)	0.56	0.16	0.30	0.68	−0.05	1.00	
d_1	−0.0877(56)	−0.13	−0.43	0.28	0.08	−0.34	0.09	1.00
d_2	[0.0]							
N	65							
σ	104							
χ_+	−1.543 (21)	1.00						
χ_-	−5.777 (26)	−0.38	1.00					
N	16							
N_{spl}	31							
σ	17							
$\overline{\Delta\nu_{hfs}}$	695							
χ_{aa}	1.543 (21)							
χ_{bb}	−3.660 (24)							
χ_{cc}	2.117 (24)							

Table 3b. 4-Methyl oxazole.

		Correlation matrix							
A	9242.2714(87)	1.00							
B	3529.6374(33)	0.89	1.00						
C	2594.7319(26)	0.82	0.81	1.00					
D_J	0.266 (11)	0.76	0.73	0.65	1.00				
D_{JK}	2.005 (65)	0.68	0.62	0.51	0.68	1.00			
D_K	2.94 (11)	0.50	0.36	0.30	0.76	0.16	1.00		
d_1	−0.0859(55)	−0.58	−0.62	−0.33	−0.75	−0.85	−0.40	1.00	
d_2	0.0035(33)	0.49	0.47	0.36	0.64	0.86	0.26	−0.93	1.00
N	88								
σ	112								
χ_+	−0.689 (10)	1.00							
χ_-	−5.287 (12)	−0.26	1.00						
N	15								
N_{spl}	31								
σ	9								
$\overline{\Delta\nu_{hfs}}$	597								
χ_{aa}	0.689 (10)								
χ_{bb}	−2.988 (11)								
χ_{cc}	2.299 (11)								

Table 3c. 5-Methyl oxazole. The three fourth order centrifugal distortion paramters D_J, D_K and d_2 had to be restricted to zero.

		Correlation matrix				
A	9304.8122(81)	1.00				
B	3579.3533(16)	0.27	1.00			
C	2626.8484(15)	0.12	0.40	1.00		
D_{JK}	2.246 (35)	0.87	0.15	−0.01	1.00	
d_1	−0.1102(22)	−0.10	−0.53	0.48	−0.16	1.00
N	55					
σ	62					
χ_+	2.215 (13)	1.00				
χ_-	−2.617 (10)	0.07	1.00			
N	19					
N_{spl}	37					
σ	8					
$\overline{\Delta\nu_{hfs}}$	328					
χ_{aa}	−2.220 (13)					
χ_{bb}	−0.201 (12)					
χ_{cc}	2.416 (12)					

Table 4. Internal rotation parameters of 2-, 4- and 5-methyl oxazole. $w_1(s)$: first Fourier coefficient, $\measuredangle(a,i)$, $\measuredangle(b,i)$: angle between the inertia axis a resp. b and the internal rotation axis i, I_α: moment of inertia of the methyl group, N: number of rotational lines, N_{spl}: number of torsional splittings used for internal rotation IAM analysis, σ: standard deviation of the fit, $\overline{\Delta\nu_{AE}}$: arithmetic mean of the experimental torsional splittings, s: reduced barrier height, V_3: barrier hindering internal rotation of the methyl group (V_3 is given in cal/mol and in kJ/mol using the relation 1 kJ = 4.18674 · 10^{-3} cal.), F: reduced rotational constant of the internal rotation, λ_a, λ_b: direction cosines of the internal rotation axis i (cosines of $\measuredangle(a,i)$ and $\measuredangle(b,i)$); standard errors in units of the last digit in brackets, derived parameters below the line.

Table 4a. 2-Methyl oxazole.

			Correlation matrix		
$w_1(s)$		$-0.4950(15)\cdot10^{-2}$	1.00		
$\measuredangle(a,i)$	[°]	5.7 (16)	−0.99	1.00	
I_α	[amuÅ^2]	3.201 (13)	−0.95	0.95	1.00
N		24			
N_{spl}		24			
σ	[kHz]	533			
$\overline{\Delta\nu_{AE}}$	[MHz]	139.743			
s		20.036(17)			
V_3	[cal/mol]	720.0 (35)			
V_3	[kJ/mol]	3.014(15)			
F	[GHz]	167.52 (68)			
$\measuredangle(b,i)$	[°]	84.3 (16)			
λ_a		0.9951(32)			
λ_b		0.099(28)			

Table 4b. 4-Methyl oxazole.

			Correlation matrix		
$w_1(s)$		$-0.50279(57)\cdot10^{-3}$	1.00		
$\measuredangle(a,i)$	[°]	4.76 (68)	−0.99	1.00	
I_α	[amuÅ^2]	3.2007 (52)	−0.91	0.91	1.00
N		38			
N_{spl}		40			
σ	[kHz]	73			
$\overline{\Delta\nu_{AE}}$	[MHz]	57.562			
s		34.0191(77)			
V_3	[cal/mol]	1223.7 (23)			
V_3	[kJ/mol]	5.1233(96)			
F	[GHz]	167.67 (27)			
$\measuredangle(b,i)$	[°]	85.24 (68)			
λ_a		0.9966(11)			
λ_b		0.083 (12)			

Table 4c. 5-Methyl oxazole.

			Correlation matrix		
$w_1(s)$		$-0.29111(83)\cdot10^{-3}$	1.00		
$\measuredangle(a,i)$	[°]	5.12 (16)	−0.69	1.00	
I_α	[amuÅ^2]	3.1848 (69)	0.92	−0.39	1.00
N		17			
σ	[kHz]	4			
$\overline{\Delta\nu_{AE}}$	[MHz]	2.038			
s		37.793 (20)			
V_3	[cal/mol]	1366.3 (37)			
V_3	[kJ/mol]	5.720 (15)			
F	[GHz]	168.52 (37)			
$\measuredangle(b,i)$	[°]	84.88 (16)			
λ_a		0.9960(3)			
λ_b		0.0892(28)			

For an optimization of structural parameters we accepted the r_s-structure of oxazole [1] without alteration for the methyl isomers, assumed a plausible methyl group structure (an ideal tetrahedral configuration with the angle $\measuredangle(HCH) = 109.47°$ and a C−H distance of 1.088 Å), and with an r_0-structure calculation fitted the distance between oxazole ring carbon and methyl carbon atom to the three rotational constants of each methyl derivative. We carried out a series of such fits gradually varying the angle between oxazole ring and methyl group, until we arrived at the angle $\measuredangle(a,i)$ we had obtained by IAM torsional analysis (see above). Since we merely get the cosine of $\measuredangle(a,i)$ out of this internal rotation fit, i.e., an absolute figure without sign, we could arrive at a positive or a negative angle $\measuredangle(a,i)$ with our r_0-structure fits. Of these two possible cases we decided to take that with the smallest methyl-ring angle deviation from oxazole. After this choice the methyl-ring C−C distances turned out to be 1.519 Å, 1.527 Å, and 1.514 Å for 2-, 4-, and 5-methyl oxazole respectively. If one now puts the principal coupling tensor, as it is known from oxazole [2], into this final structure, one gets angles $\measuredangle(z,a)$ between the principal tensor z- and the principal inertial a-axis. These angles are graphically displayed in Fig. 2 for the three methyl-oxazoles.

The projections χ_{aa} and χ_{bb} were then calculated according to

$$\chi_{aa} = \chi_{xx}\cdot\sin^2\{\measuredangle(z,a)\} + \chi_{zz}\cdot\cos^2\{\measuredangle(z,a)\}, \quad (1a)$$

$$\chi_{bb} = \chi_{xx}\cdot\cos^2\{\measuredangle(z,a)\} + \chi_{zz}\cdot\sin^2\{\measuredangle(z,a)\}, \quad (1b)$$

and are shown in Fig. 3 as sine curves dependent on $\measuredangle(z,a)$ in the range $-90° \leqq \measuredangle(z,a) \leqq 90°$. The three methyl derivatives and their parent mole-

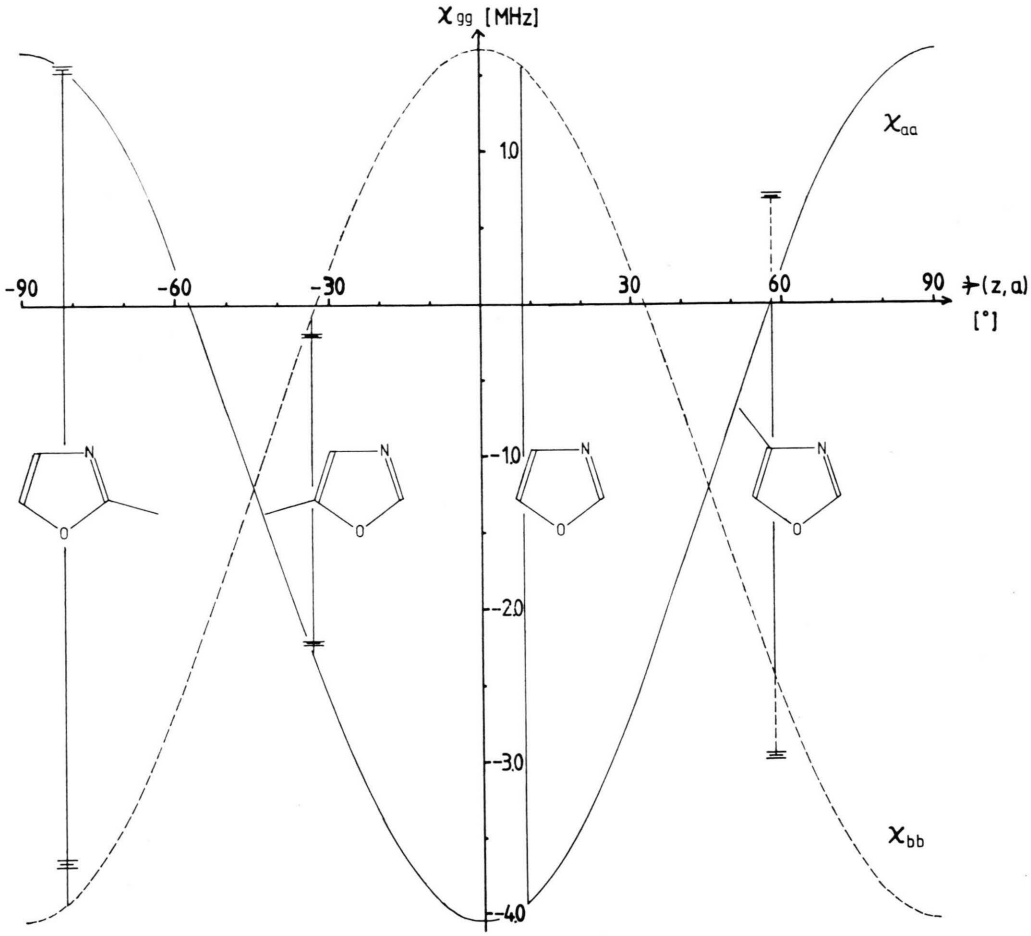

Fig. 4. Graphic comparison of ^{14}N-hfs coupling constants χ_{aa} and χ_{bb} obtained by projecting the principal coupling tensor elements χ_{xx} and χ_{zz} of oxazole [2] on the principal inertia axes a and b of the respective methyl oxazole, with the experimental values from a ^{14}N-hfs analysis. – The inertia axes a and b were fixed with an r_0 structural analysis assuming that the heterocyclic ring structure [1] did not change under methyl substitution. $\measuredangle(z, a)$ (see Fig. 3) range was confined to $-90° \leqq \measuredangle(z, a) \leqq 90°$. ≡: Experimental χ_{aa} and χ_{bb} values with single standard error limits.

molecule, oxazole, are drawn in as vertical bars with their $\measuredangle(z, a)$- and experimentally determined χ_{aa}- and χ_{bb}-values, which for oxazole coincide with the points of intersection with the sine curves.

With the exception perhaps of 4-methyl oxazole, it can be stated that from structure and oxazole parent expected and experimentally obtained $\chi_{gg}(g = a, b)$-values are in good agreement. The quadrupole coupling tensor is proportional by the nuclear quadrupole moment eQ as a factor to the tensor of the second derivatives of the electric potential thus providing information about the electronic environment at the quadrupole nucleus. When measuring the first ^{14}N-hfs patterns with MWFT spectroscopy, we had already made use of this result roughly calculating provisional coupling constants to confirm the assignment of these first lines. Deviations of experiment and expectation (sine curves) are to some extent due to uncertainties in structure calculations. To sum up, the graphic comparison in Fig. 4 shows that methyl substitution exerts little influence on the principal ^{14}N quadrupole coupling tensor.

When looking at the centrifugal distortion results, one realizes that with the exception of D_K the centrifugal distortion constants are of the same order of magnitude for the three methyl oxazoles. This may be explained by the fact that the atoms

constituting the heterocyclic ring all stem from the first row of the periodic classification and that, because of this rather homogeneous distribution of masses and the relatively wide spacing of ring and methyl group, the orientation of the inertial *a*-axis is determined by and nearly collinear with the methyl alignment.

Viewing the torsional analysis data, two observations have to be put on record. Within standard errors, the moment of inertia of the methyl group, I_α, turns out to be the same in all three cases. Secondly, the barrier hindering methyl internal rotation is significantly lower for 2-methyl oxazole compared to 4- and 5-methyl oxazole. An explanation of this rather low barrier could be that in 4- and 5-methyl oxazole we find an H-atom with approximately double van der Waals-distance to the methyl H-atoms at the neighbouring ring position, whereas in 2-methyl oxazole both neighbouring positions are occupied by the two heteroatoms. An attracting interaction between methyl H-atoms and lone electron pairs at N and O seems to be rather unfavourable because of the resulting tensed four-membered ring so that the observed difference in hindering potentials may be due to steric interaction of ring and methyl H-atoms.

Acknowledgements

We thank the members of our group for assistance and helpful advice. We are further gratefully indebted to the Deutsche Forschungsgemeinschaft and Fonds der Chemie for granting funds. The necessary computer facilities were made available by the Rechenzentrum der Christian-Albrechts-Universität zu Kiel.

The work at Bangor was supported by grants from the Science and Engineering Research Council, U.K., and K.I. thanks the University College of North Wales for the award of a Sir William Roberts Scholarship. Initial assignments for 4-methyl oxazole were made by J.S. at the Chemistry Department of the University of Texas at Austin, and we are grateful to Dr. James E. Boggs for the provision of facilities and to the University of Texas for financial support. J.S. also thanks the Royal Society and the University College of North Wales for support while on leave at Kiel during the initiation of this collaboration.

[1] A. Kumar, J. Sheridan, and O. L. Stiefvater, Z. Naturforsch. **33a,** 145 (1978).
[2] A. Kumar, J. Sheridan, and O. L. Stiefvater, Z. Naturforsch. **33a,** 549 (1978).
[3] K. Iqbal, doctoral thesis, University College of North Wales, Bangor 1979.
[4] E. Fliege, H. Dreizler, J. Sheridan, and C. T. Walls, J. Mol. Spectrosc. **113,** 362 (1985).
[5] J. W. Cornforth and R. H. Cornforth, J. Chem. Soc. **1953,** 96.
[6] R. Schröder, U. Schöllkopf, E. Blume, and I. Hoppe, Liebigs Ann. Chem. **1975,** 533.
[7] G. Bestmann, H. Dreizler, E. Fliege, and W. Stahl, J. Mol. Struct. **97,** 215 (1983).
[8] G. Bestmann and H. Dreizler, Z. Naturforsch. **37a,** 58 (1982).
[9] G. Bestmann, H. Dreizler, H. Mäder, and U. Andresen, Z. Naturforsch. **35a,** 392 (1980).
[10] T. Ogata and K. Kozima, Bull. Chem. Soc. Japan **44,** 2344 (1971).
[11] T. Ogata and K. Kozima, J. Mol. Spectrosc. **42,** 38 (1972).
[12] V. Typke, J. Mol. Spectrosc. **63,** 170 (1976).
[13] J. K. G. Watson, in: Vibrational Spectra and Structure (J. R. Durig, ed.), Vol. 6, pp. 42–45, Elsevier, New York 1977.
[14] R. C. Woods, J. Mol. Spectrosc. **21,** 4 (1966).
[15] R. C. Woods, J. Mol. Spectrosc. **22,** 49 (1967).